Reprint ISSN 0973-9424

International Journal Of Mathematical Sciences And Engineering Applications

(IJMSEA)

ASCENT PUBLICATION
@
ASCENT
PUNE, INDIA

www.ascent-journals.com

International J. of Math. Sci. & Engg. Appls. (IJMSEA)
ISSN 0973-9424, Vol. 13 No. II (December, 2019), pp. 1-16

INFLUENCE OF MHD WITH RADIATION, CHEMICAL REACTION AND SORET EFFECTS ON FREE CONVECTIVE HEAT AND MASS TRANSFER FLOW THROUGH A HIGHLY POROUS MEDIUM

TEJ SINGH[1] AND HEMANT PAL[2]
[1] Department of Mathematics, Government College Chamba,
Distt. Chamba, Himachal Pradesh-176314, India
[2] Department of Physics,Government College Chamba,
Distt. Chamba, Himachal Pradesh-176314, India

Abstract

In the present study, the influence of MHD with radiation, chemical reaction and soret effects on free convective heat and mass transfer flow through a highly porous medium is critically analyzed. A gray, absorbing and emitting but non-scattering medium is considered for this study. A uniform magnetic field is considered in a direction normal to the plate. The governing equations for this investigation are formulated and transformed into a set of ordinary differential equations using non-dimensional parameters. The perturbation technique is used to solve these equations analytically. The effects of various parameters on the velocity, temperature, concentration, skin-friction coefficient, Nusselt number and Sherwood number are tabulated and analyzed graphically. It reveals that velocity distribution decreases with increasing magnetic field parameter; temperature decreases with increasing Prandtl number and concentration decreases with increasing the Schmidt number and chemical reaction parameter.

—————————————————————————————

Key Words : *MHD, Soret, Thermal radiation, Free convection, Chemical Reaction, Heat source, Highly porous.*

1. Introduction

In recent years, the analysis of magnetic hydro dynamic (MHD) convection flow involving heat and mass transfer in porous medium has drawn the attention of many scholars because of its possible applications in diverse fields such as astrophysics, soil-sciences, geophysics, nuclear power reactors etc. It is also used in designing of accelerators, MHD generators and underground water energy storage system etc. It is important to elucidate that MHD is now undergoing a stage of great differentiation and enlargement of the subject matter. These new problems have also attracted attention of the researchers due to its varied significance, in ionized gases, liquid metals and electrolytes etc. The present status of MHD study is due to contributions of several prominent research scholars like Shercliff [1], Ferraro and Plumpton [2] and Crammer and Pai [3]. Raptis [4] studied the presence of a magnetic field through a porous medium. K.D. Singh [5] has also critically analyzed the MHD effects on the three-dimensional flow through a porous plate. N. K. Varshney and Ram Prakash [8] examined the MHD effect on three dimensional free convective flows with heat transfer through a porous medium with periodic permeability. K. Jhansi Rani et. al. [10] proposed the heat and mass transfer effects on MHD free convection flow over an inclined plate embedded in a porous medium.

Ashish Paul [11] derived the transient free convective MHD flow passing an exponentially accelerated vertical porous plate with variable temperature through a porous medium. K. Suneetha et. al. [13] examined the effect of free convective heat and mass transfer flow through a highly porous medium with radiation, chemical reaction and soret effects. A combined effect of slip parameter and inclined magnetic field on MHD flow through two infinite parallel plates filled by porous medium was presented by K. Ramakrishnan [14].

In the present paper an attempt has been made to study the influence of MHD with radiation, chemical reaction and soret effects in free convective heat and mass transfer flow through a highly porous medium in the presence of magnetic field.

2. Mathematical Analysis

Here in this study an unsteady two-dimensional laminar free convective mass transfer flow of a viscous incompressible fluid through a highly porous medium passing an infinite vertical moving porous plate in the presence of heat generating thermal radiation with chemical reaction and Soret effect is critically analyzed. The fluid as well as the porous structure is assumed to be in local thermal equilibrium. It is also assumed that the radiations are only coming from the fluid (M.Q. Brevster [6], A. Raptis and C. Perdikis [7] and B. Shankar Goud and M.N. Raja Shekar [12]). Here the fluid medium is considered as a gray, emitting and absorbing but non-scattering. Rosseland approximation is applied to describe the radiative heat flux in the energy equation. As the rate of chemical reaction is directly proportional to the species concentration a homogeneous first-order chemical reaction between the fluid and species concentration is considered. All the fluid properties are assumed to be constant except that the influence of the density variation with temperature is considered only in the body force term (Boussinesqs approximation) (S.M. Ibrahim [9], A. Raptis and C. Perdikis [7] and B. Shankar Goud and M.N. Raja Shekar [12]). Hence under the usual Boussinesqs approximation, the continuity mass equation [Eq. (1)], linear momentum [Eq. (2)], energy [Eq. (3)], and diffusion [Eq. (4)] are respectively as follows.

$$\frac{\partial v^*}{\partial y^*} = 0 \tag{1}$$

$$\frac{\partial u^*}{\partial t^*} + V^* \frac{\partial u^*}{\partial y^*} = -\frac{1}{\rho}\frac{\partial p^*}{\partial x^*} + \vartheta \frac{\partial^2 u^*}{\partial y^{*2}} + g\beta(T^* - T^*_\infty) + g\beta^*(C^* - C^*_\infty) - \frac{\sigma B_0^2 u^*}{\rho} - \frac{\vartheta}{k^*}\varphi u^* \tag{2}$$

$$\sigma\frac{\partial T^*}{\partial t^*} + \varphi v^* \frac{\partial T^*}{\partial y^*} = \frac{k}{\rho C_p}\frac{\partial^2 T^*}{\partial y^{*2}} - \frac{\varphi}{\rho c_p}\frac{\partial q_r}{\partial y^*} + \frac{Q_0}{\rho c_p}(T^* - T^*_\infty) \tag{3}$$

$$\frac{\partial C^*}{\partial t^*} + v^* \frac{\partial C^*}{\partial y^*} = D\frac{\partial^2 C^*}{\partial y^{*2}} - Kr^*(C^* - C^*_\infty) + D_1 \frac{\partial^2 T^*}{\partial y^{*2}}. \tag{4}$$

The x^*-axis is chosen along the plate in the direction opposite to the direction of gravity and the y^*- axis is taken normal to it. A uniform magnetic field B_0 is applied in a direction parallel to the y* axis. As shown in Fig. 1. Since the flow field is of extreme size, all the variables are functions of y and t only.

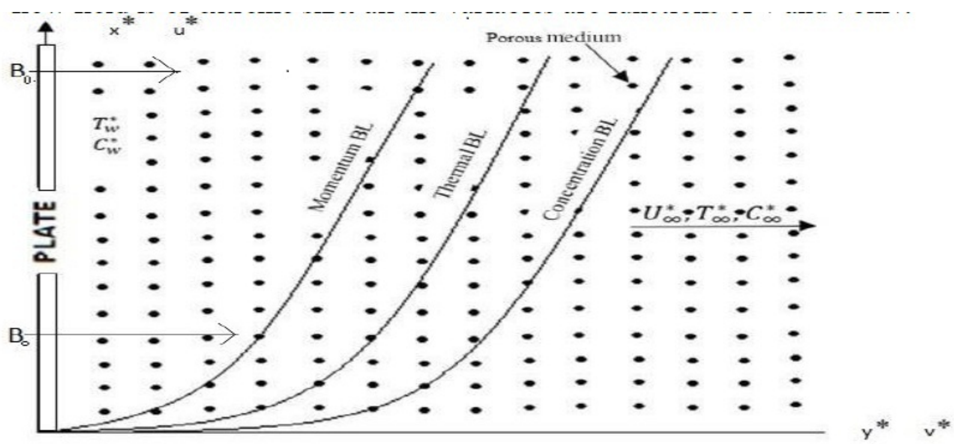

Fig. 1. Flow configuration of the problem.

where x^*, y^* and t^* are the dimensional distances along and perpendicular to the plate and dimensional time, respectively; u^* and v^* are the components of dimensional velocities along x^* and y^* directions, respectively; C^* and T^* are the dimensional concentration and temperature of the fluid, respectively; ρ is the fluid density; ϑ is the kinematic viscosity; C_p is the specific heat at constant pressure; σ is the heat capacity ratio; g is the acceleration due to gravity; β and β^* are the volumetric coefficient of thermal and concentration expansion; k^* is the permeability of the porous medium; φ is the porosity; D is the molecular diffusivity; Kr^* is the chemical reaction parameter; k is the fluid thermal conductivity, and D_1 is the Soret number. The third, fourth and fifth terms on the right-hand side of the momentum [Eq. (2)] denote the thermal, concentration buoyancy and magnetic field effects, respectively, and the sixth term represents the bulk matrix linear resistance, that is, Darcy term. Also, the second term on the right-hand side of the energy [Eq. (3)] represents thermal radiation. The radiative heat flux term by using the Resseland approximation [M.Q. Brevster [6]], is given by:

$$q_r = \frac{-4\sigma_S}{3k_e}\frac{\partial T^{*4}}{\partial y^*} \tag{5}$$

where σ_S the Stefan-Boltzman is constant and k_e is the men absorption coefficient. It should be noted that by using the Resseland approximation, the present analysis is limited to optically thick fluids. It was assumed that the temperature difference within the flow is sufficiently small such that T^4 may be expressed as a linear function of the temperature. This is accomplished by expanding in a Taylor series about T_∞ and neglecting higher-order terms, thus:

$$T^{*4} \cong 4T_{\infty}^{*3}T^{*} - 3T_{\infty}^{*4}. \tag{6}$$

It is assumed that the permeable plate moves with constant velocity in the direction of fluid flow. It is also assumed that the plate temperature and concentration are exponentially varying with time. Under these assumptions, the appropriate boundary conditions for the velocity, temperature, and concentration fields are:

$$u^* = U_p^*, T* = T_w^* + \epsilon(T_w^* - T_\infty^*)e^{n^*t^*}, C^* = C_w^* + \epsilon(C_w^* - C_\infty^*)e^{n*t^*} \quad \text{at} \quad y^* = 0,$$

$$u^* \to U_\infty^*,\ T^* \to T_\infty^*, C^* \to C_\infty^* \quad \text{as} \quad y^* \to \infty \tag{7}$$

where U_p^* is the wall dimensional velocity; C_w^* and T_w^* are the wall dimensional concentration, and temperature, respectively; U_∞^*, C_∞^* and T_∞^* are the free stream dimensional velocity, concentration and temperature, respectively; and n^* is the constant.
It is clear from Eq. (1) that the suction velocity normal to the plate is either a constant or a function of time. Hence the suction velocity normal to the plate is taken as:

$$v^* = -v_0 \tag{8}$$

where v_0 is a scale of suction velocity which is a nonzero positive constant. The negative sign indicates that the suction is towards the plate. Outside the boundary layer, Eq. (2) gives:

$$\frac{1}{\rho}\frac{dp^*}{dx^*} = -\frac{\varphi^\vartheta}{K^*}U_\infty^*. \tag{9}$$

To render dimensionless solutions and facilitate analytical analysis, the following dimensionless variables are defined:

$$u = \frac{u^*}{U_\infty^*},\ y = \frac{y^*v_0}{\vartheta},\ U_p = \frac{U_p^*}{U_\infty^*},\ M = \frac{\sigma B_0^2\vartheta}{pv_0^2},\ n = \frac{n^*\vartheta}{v_0^2},$$

$$t = \frac{t^*v_0^2}{\vartheta}, \quad \lambda = \frac{\sigma}{\varphi}, \quad \theta = \frac{T^* - T_\infty^*}{T^w - T_\infty^*}, \quad C = \frac{C^* - C_\infty^*}{C_w^* - C_\infty^*}. \tag{10}$$

In view of Eqs. (5-10), Eqs. (2-4) are reduced to the following non-dimensional form:

$$\frac{\partial u}{\partial t} - \frac{\partial u}{\partial y} = \frac{\partial^2 u}{\partial y^2} + Gr\ \theta + GcC - Mu + \frac{1}{k}(1-u) \tag{11}$$

$$\lambda\,\frac{\partial\theta}{\partial t}-\frac{\partial\theta}{\partial y}=\frac{1}{r}\frac{\partial^2\theta}{\partial y^2}+Q\theta \tag{12}$$

$$\frac{\partial C}{\partial t}-\frac{\partial C}{\partial y}=\frac{1}{Sc}\frac{\partial^2 C}{\partial y^2}-KrC+So\frac{\partial^2\theta}{\partial y^2}. \tag{13}$$

The corresponding dimensionless boundary conditions are:

$$u=U_p,\quad \theta=1+\epsilon e^{nt},\ C=1+\epsilon e^{nt}\ \text{ at }\ y=0$$

$$u\to 1,\quad \theta\to 0,\quad C\to 0\ \text{ as }\ y\to\infty \tag{14}$$

where $r=\frac{3RPr}{3R+4}$ and $Gr=\frac{g\beta\vartheta(T_w^*-T_\infty^*)}{U_\infty^* v_0^2}$ are the thermal Grashof numbers, $Gc=\frac{g\beta^*\vartheta(C_w^*-C_\infty^*)}{U_\infty^* v_0^2}$ is the solutal Grashof number, $k=\frac{k^* v_0^2}{\varphi\vartheta^2}$ is the permeability of porous parameter, $Pr=\frac{\rho C_p\varphi\vartheta}{k}$ is the Prandtl number, $R=\frac{k_e k}{4\varphi\sigma_s T_\infty^3}$ is the thermal radiation parameter, $Q=\frac{Q_0 v}{\varphi\rho C_p v_0^2}$ is the heat source parameter, $Sc=\frac{\vartheta}{D}$ is the Schmidt number, $Kr=\frac{Kr^*\vartheta}{v_0^2}$ is the chemical reaction parameter and $So=\frac{D_1(T_w^*-T_\infty^*)}{\vartheta(C_w^*-C_\infty^*)}$.

3. Solution of the Problem

Eqs. (11-13) are coupled; these equations and nonlinear partial differential equations cannot be solved in closed form. However, these equations can be reduced to a set of ordinary differential equations, which can be solved analytically. This can be done by representing the velocity, temperature, and concentration of the fluid in the neighborhood of the plate as:

$$\begin{aligned} u(y,t) &= u_0(y)+\epsilon e^{nt}u_1(y)+o(\epsilon)^2+\cdots \\ \theta(y,t) &= \theta_0(y)+\epsilon e^{nt}\theta_1(y)+o(\epsilon)^2+\cdots \\ C(y,t) &= C_0(y)+\epsilon e^{nt}C_1(y)+o(\epsilon)^2+\cdots \end{aligned} \tag{15}$$

Substituting Eq. (15) in Eqs. (11-13), equating the harmonic and non-harmonic higher order terms of $o(\epsilon)^2$, the following equations can be obtained:

$$\begin{gathered} u_0''+u_0'-\frac{1}{k}(1+M)u_0=-\frac{1}{k}-Gr\theta_0-GcC_0 \\ u_1''+u_1'-M_1u_1=-Gr\theta_1-GcC_1 \\ \theta_0''+\kappa\theta_0'+\kappa\theta_0 Q=0 \\ \theta_1''+\kappa\theta_1'+\kappa M_2\theta_1=0 \end{gathered} \tag{16}$$

$$C_0^{''} + ScC_0' - ScKrC_0 = -ScS0\theta_0^{''}$$

$$C_1^{''} + ScC_1' - ScM_3C_1 = ScSo\theta_1^{''}$$

where $M_1 = n + M + \frac{1}{k},\ M_2 = Q - n\lambda,\ M_3 = Kr + n.$

The prime denotes ordinary differentiation with respect to y. The corresponding boundary conditions can be written as:

$$u_0 = U_p, u_1 = 0,\ \theta_0 = 1,\ \theta_1 = 1,\ C_0 = 1, C_1 = 1 \quad \text{at} y = 0 \quad \text{and}$$

$$u_0 \to 1, u_1 \to 0, \theta_0 = 0, \theta_1 = 0, C_0 \to 0, C_1 \to 0 \quad \text{as} \quad y \to \infty. \tag{17}$$

Solving Eq. (16) subject to boundary conditions of Eq. (17), the velocity, temperature, and concentration distributions in the boundary layer can be obtained as:

$$\begin{aligned} u(y,t) &= (M_{12}e^{-r_{10}y} + M_{13}e^{-r_2y} - M_{10}e^{-r_6y} + M_8) \\ &\quad +\epsilon e^{nt}(M_{17}e^{-r_{12}y} + M_{18}e^{-r_4y} - M_{12}e^{-r_3y}) \end{aligned} \tag{18}$$

$$\theta(y,t) = e^{-r_2y} + \epsilon e^{nt}(e^{-r_4y}) \tag{19}$$

$$C(y,t) = (M_5e^{-r_6y} - M_4e^{-r_2y}) + \epsilon e^{nt}(M_7e^{-r_8y} - M_6e^{-r_4y}) \tag{20}$$

where the expressions for the constants are given in the appendix.

The skin-friction, Nusselt number, and Sherwood number are important physical parameters for this type of boundary layer flow. These parameters can be defined and determined as follows:

Knowing the velocity field, skin-friction at the plate can be obtained, which in non-dimensional form is given by:

$$\begin{aligned} \frac{\tau^*}{\rho U_0 v_0} &= \left(\frac{\partial u}{\partial y}\right)_{y=0} = \left(\frac{\partial u_0}{\partial y} + \epsilon e^{nt}\frac{\partial u_1}{\partial y}\right)_{y=0} \\ &= (-r_{10}M_{12} - r_2M_{13} + r_6M_{10}) + \epsilon e^{nt}(-r_{12}M_{17} - r_4M_{18} + r_8M_{15}). \end{aligned} \tag{21}$$

Knowing the temperature field, the rate of heat transfer coefficient can be obtained, which in the non-dimensional form, in term of the number, is given by:

$$\begin{aligned} Nu &= -x\frac{\left(\frac{\partial T}{\partial y^*}\right)_{y^*=0}}{(T_2^* - T_\infty^*)} \Rightarrow NuRe_x^{-1} = -\left(\frac{\partial \theta}{\partial y}\right)_{y=0} = -\left(\frac{\partial \theta_0}{\partial y} + \epsilon e^{nt}\frac{\partial \theta_1}{\partial y}\right)_{y=0} \\ &= r_2 + \epsilon e^{nt} r_4. \end{aligned} \tag{22}$$

Knowing the concentration field, the rate of mass transfer coefficient can be obtained, which in the non-dimensional form, in terms of the Sherwood number, is given by:

$$\begin{aligned} Sh &= -x\frac{\left(\frac{\partial C}{\partial y^*}\right)_{y^*}}{(C_w^*-C_\infty^*)} \Rightarrow ShRe_x^{-1} = -\left(\frac{\partial C}{\partial y}\right)_{y=0} = -\left(\frac{\partial C_0}{\partial y} + \epsilon e^{nt}\frac{\partial C_1}{\partial y}\right)_{y=0} \\ &= (r_6M_5 - r_2M_4) + \epsilon e^{nt}(r_8M_7 - r_4M_6) \end{aligned} \tag{23}$$

where $Re_x = \frac{v_0 x}{v}$ is the local Reynolds number.

4. Results and Discussion

The system of ordinary differential Eq. (16) with boundary conditions of Eq. (17) is solved analytically by employing the Perturbation technique. The solutions are obtained for the steady and unsteady velocity, temperature, and concentration fields from the Eqs. (18-20).The expressions obtained in previous section are studied with the help of graphs from Figs. 2- 10 and Tables 1-3. The effects of various physical parameters viz., the thermal Grashof number Gr, the solutal Grashof number Gc, Prandtl number Pr, Schmidt number Sc, the radiation parameter R, the permeability of the porous medium k, the heat generation parameter Q, the chemical reaction parameter Kr, and the Soret number So. In the present study, the default parametric values are adopted as: $Gr = 2.0, Gc = 2.0, k = 5.0, \lambda = 1.4, Sc = 0.2, R = 5.0, Kr = 2.0, Q = 0.1, Pr = 0.71, So = 0.5, Up = 0.4, n = 0.1, t = 1.0, M = 1$ and $\epsilon = 0.01$.

Table 1 : Effect of various physical parameter on Skin friction for $k = 5.0, Q = 0.1, \lambda = 1.4, Pr = 0.71, R = 5.0, Sc = 0.2, Kr = 2.0, So = 0.5, Up = 0.4, M = 1$ values.

Gr	Gc	K	Cf	Nu	Sh
2.0	2.0	5.0	4.83835	0.43686	0.72925
3.0	2.0	5.0	6.19189	0.43686	0.72925
4.0	2.0	5.0	7.545423	0.43686	0.72925
2.0	3.0	5.0	7.66833	0.43686	0.72925
2.0	4.0	5.0	6.448831	0.43686	0.72925
2.0	2.0	6.0	8.026023	0.43686	0.72925
2.0	2.0	7.0	7.302809	0.43686	0.72925

Table 2 : Effect of various physical parameter on Skin friction for $Gr = 2.0, Gc = 2.0, k = 5.0, \ = 1.4, Sc = 0.2, Kr = 2.0, So = 0.5, Up = 0.4, M = 1$ values.

Pr	R	Q	Cf	Nu	Sh
0.71	5.0	0.1	4.83835	0.43686	0.72925
1.0	5.0	0.1	4.188243	0.681138	0.710865
1.5	5.0	0.1	3.616305	1.087459	0.676287
0.71	6.0	0.1	4.760776	0.459379	0.727678
0.71	7.0	0.1	4.705379	0.47633	0.726477
0.71	5.0	0.01	4.469282	0.557739	72049
0.71	5.0	0.015	4.483183	0.55246	0.720891

Table 3 : Effect of various physical parameter on Skin friction for $Gr = 2.0, Gc = 2.0, k = 5.0, Q = 0.1, \ = 1.4, Pr = 0.71, R = 5.0, Up = 0.4, M = 1$ values.

Sc	Kr	So	Cf	Nu	Sh
0.2	2.0	0.5	4.83835	0.43686	0.72925
0.3	2.0	0.5	4.538905	0.436855	0.923133
0.4	2.0	0.5	4.342326	0.436855	1.096216
0.2	3.0	0.5	4.599168	0.436855	0.995847
0.2	4.0	0.5	4.437979	0.436855	0.995847
0.2	2.0	0.6	4.848322	0.436855	.725364
0.2	2.0	0.7	4.862741	0.436855	0.721485

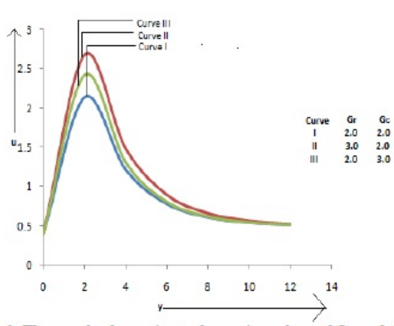

Fig. 2. The graph of u against y for varies values of Gr and Gc.

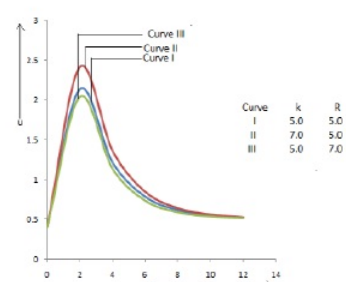

Fig. 3. The graph of u against y for varies values of k and R.

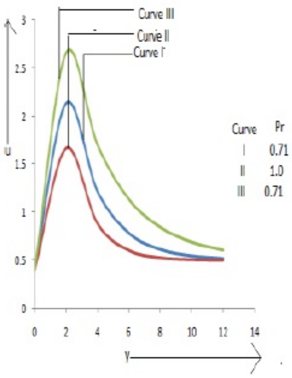

Fig. 4. The graph of u against *y* for varies values of Pr and Q.

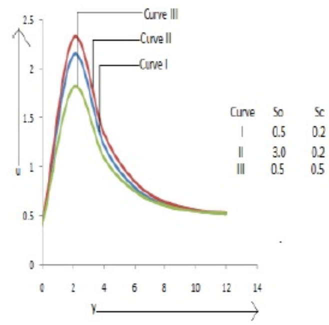

Fig. 5. The graph of u against y for varies values of So and *Sc*.

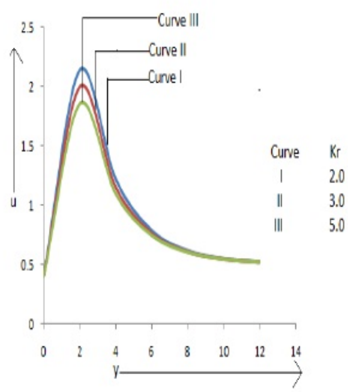

Fig. 6. The graph of u against y for varies values of *Kr*.

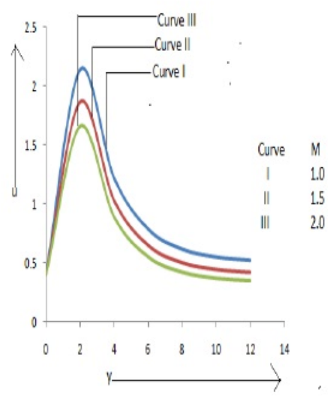

Fig. 7. The graph of u against y for varies values of M.

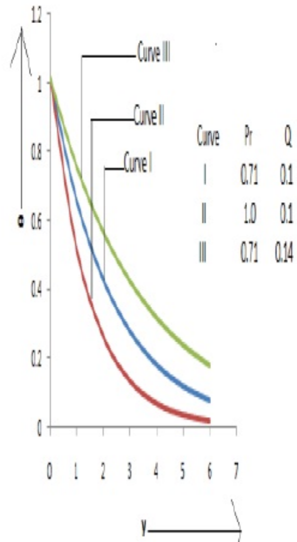

Fig. 8. The graph of θ against y for varies values of Pr and Q.

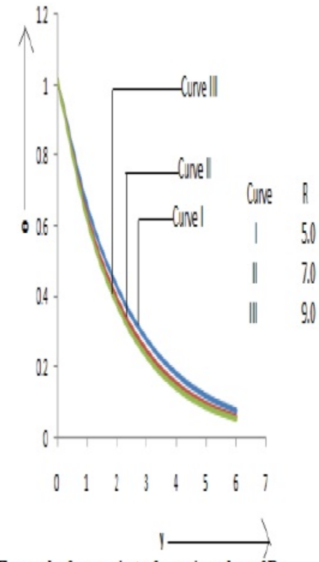

Fig. 9. The graph of Θ against y for varies values of R.

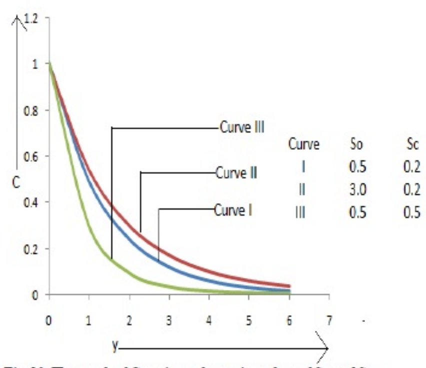

Fig. 10. The graph of C against y for varies values of So *and* Sc.

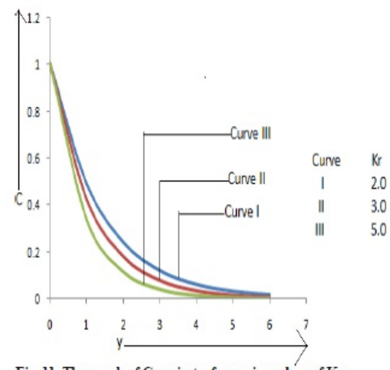

Fig. 11. The graph of C against y for varies values of Kr.

The thermal Grashof number Gr gives the relative effect of the thermal buoyancy force to the viscous hydrodynamic force in the boundary layer. The solutal Grashof number Gc is the ratio of the species buoyancy force to the viscous hydrodynamic force. It is due to the fact that the increase in the value of Gr and the Gc has the tendency to increase the thermal and mass buoyancy effect. The fig. 2 shows the effect of Gr and Gc on the velocity field and it is find that greater cooling of the surface leads to an increase in Gr, and Gc results in an increase in the velocity.

The R defines the relative contribution of conduction heat transfer to thermal radiation transfer. Fig.3. represents the effect of the permeability of the porous medium k, and the radiation parameter R on the velocity field. It is evident from the figure that with

the increase of k velocity increases, while it is decreases with the increase of R.
Figs. 4 and 8, represents the effect of Pr and Q on the velocity and temperature fields. From these figures it is observed that velocity and temperature decreases when Pr increases, whereas they increase when Q increases. The reason is that the conductivity of the fluid and therefore heat is able to diffuse away from the heated surface more rapidly for higher values of Pr. Hence in the case of smaller Pr, the thermal boundary layer is thicker and the rate of heat transfer is reduced.
The Sc embodies the ratio of the momentum to the mass diffusivity. It, therefore, quantifies the relative effectiveness of the momentum and mass transport by diffusion in the hydrodynamic (velocity) and concentration (species) boundary layers. Figs. 5 and 10 show the variation of velocity and concentration profiles for various values of Sc and So. These figures revealed that increase in the values of So increases the velocity and concentration distribution. While the increase in the values of Sc decreases the velocity and concentration distribution.
Figs. 6 and 11 show the dimensionless velocity and concentration profiles for different values of Kr. It can be seen that both velocity and the concentration profiles decreases with the increase of Kr. Fig. 7 depicts the velocity profiles for different values of M, and it is observed that an increase in the M decreases the Velocity. Fig. 9 shows the temperature profiles for different values of R, and it is seen that an increase in the R decreases the temperature.
Comparison with K. Suneetha et. al. (2018) for $Gr = 2.0, Gc = 2.0, k = 5.0, \lambda = 1.4, Sc = 0.2, R = 5.0, Kr = 2.0, Q = 0.1, Pr = 0.71, So = 0.5, Up = 0.4, n = 0.1, t = 1.0, M = 1$ **and** $\epsilon = 0.01$.

Table 4 : Effect of various physical parameter on Skin friction for $k = 5.0, Q = 0.1, \lambda = 1.4, Pr = 0.71, R = 5.0, Sc = 0.2, Kr = 2.0, So = 0.5, Up = 0.4, M = 1$ values.

			K. Suneetha et. al. (2018)			Present Result		
Gr	Gc	K	Cf	Nu	Sh	Cf	Nu	Sh
2	2	5	6.3439	0.43686	0.72925	4.83835	0.43686	0.72925
3	2	5	8.0208	0.43686	0.72925	6.19189	0.43686	0.72925
4	2	5	9.6977	0.43686	0.72925	7.545423	0.43686	0.72925
2	3	5	7.4878	0.43686	0.72925	7.66833	0.43686	0.72925
2	4	5	8.6316	0.43686	0.72925	6.448831	0.43686	0.72925
2	2	6	6.5443	0.43686	0.72925	8.016023	0.43686	0.72925
2	2	7	6.7037	0.43686	0.72925	7.302809	0.43686	0.72925

Table 5 : Effect of various physical parameter on Skin friction for $Gr = 2.0, Gc = 2.0, k = 5.0, \lambda = 1.4, Sc = 0.2, Kr = 2.0, So = 0.5, Up = 0.4, M = 1$ values.

			K. Suneetha et. al. (2018)			Present Result		
Pr	R	Q	Cf	Nu	Sh	Cf	Nu	Sh
0.71	5	0.1	6.3439	0.43686	0.72925	4.83835	0.43686	0.72925
1	5	0.1	5.4114	0.681138	0.710865	4.188243	0.681138	0.710865
1.5	5	0.1	4.6688	1.087459	0.676287	3.616305	1.087459	0.676287
0.71	6	0.1	6.2273	0.459379	0.727678	4.760776	0.459379	0.727678
0.71	7	0.1	6.1449	0.47633	0.726477	4.705379	0.47633	0.726477
0.71	5	0.01	5.8027	0.557739	0.72049	4.469282	0.557739	0.72049
0.71	5	0.015	5.8225	0.55246	0.720891	4.483183	0.55246	0.720891

Table 6 : Effect of various physical parameter on Skin friction for $Gr = 2.0, Gc = 2.0, k = 5.0, Q = 0.1, \lambda = 1.4, Pr = 0.71, R = 5.0, Up = 0.4, M = 1$ values.

			K. Suneetha et. al. (2018)			Present Result		
Sc	Kr	So	Cf	Nu	Sh	Cf	Nu	Sh
0.2	2	0.5	6.3439	0.43686	0.72925	4.83835	0.43686	0.72925
0.3	2	0.5	5.9556	0.436855	0.923133	4.538905	0.436855	0.923133
0.4	2	0.5	5.7103	0.436855	1.096216	4.342326	0.436855	1.096216
0.2	3	0.5	6.0305	0.436855	0.873937	4.599168	0.436855	0.873937
0.2	4	0.5	5.8254	0.436855	0.995847	4.437979	0.436855	0.995847
0.2	2	0.6	6.358	0.436855	0.725364	4.848322	0.436855	0.725364
0.2	2	0.7	6.3721	0.436855	0.721485	4.862741	0.436855	0.721485

The variation in the local skin-friction coefficient, local Nusselt number, and local Sherwood number for various parameters are investigated through Tables 1 - 3.
For the validity of the present work, the obtained results were compared with the available results of K. Suneetha et. al. (2018) in the absence of Magnetic field. The present result appears to be in good agreement with the results of K. Suneetha et. al. (Tables 4,5,6).

5. Conclusions

In the present study the problem of free convective heat and mass transfer flow through a highly porous medium with radiation, chemical reaction and soret effects was examined analytically in the presence of magnetic field using perturbation technique. The results obtained are in good agreement with the usual flow. A selective set of graphical results were presented and discussed to show interesting features of the flow, heat and mass transfer situation in the presence of radiation, chemical reaction, soret effect and magnetic field. It was concluded from the study that the enhanced cooling of the surface leads to an increase in Gr, and Gc which further results in an increase in the velocity. Also with the increase in value of k velocity increases but it decreases with the increase in the value of R. It also reveals that velocity and temperature varies directly with Q and inversely with Pr. Increase in the values of So, increases velocity and concentration distribution while the increase in the values of Sc, decrease the velocity and concentration distribution. The velocity and the concentration profiles decrease with the increase of Kr whereas an increase in the M decreases the velocity. Also an increase in the R results in decrease of the temperature.

Appendix

$$r_1 = \frac{-r+\sqrt{r^2-4_rQ}}{2} \qquad r_2 = \frac{-r-\sqrt{r^2-4_rQ}}{2}$$

$$r_3 = \frac{-r+\sqrt{r^2-4_rM_2}}{2} \qquad r_4 = \frac{-r-\sqrt{r^2-4_rM_2}}{2}$$

$$r_5 = \frac{-Sc+\sqrt{Sc^2+4ScKr}}{2} \qquad r_6 = \frac{-Sc-\sqrt{Sc^2+4ScKr}}{2}$$

$$r_7 = \frac{-Sc+\sqrt{Sc^2+4ScM_3}}{2} \qquad r_8 = \frac{-Sc-\sqrt{Sc^2+4ScM_3}}{2}$$

$$r_9 = \frac{-1+\sqrt{1+\frac{4(1+M)}{k}}}{2} \qquad r_{10} = \frac{-1-\sqrt{1+\frac{4(1+M)}{k}}}{2}$$

$$r_{11} = \frac{-1+\sqrt{1+4M_1}}{2} \qquad r_{12} = \frac{-1-\sqrt{1+4M_1}}{2}$$

$$M_4 = \frac{ScSor_2^2}{r_2^2-Scr_2-ScKr} \qquad M_5 = 1 + M_4$$

$$M_6 = \frac{ScSor_4^2}{r_4^2-Scr_4-ScM_3} \qquad M_7 = 1 + M_6$$

$$M_8 = \frac{1}{1+M} \qquad M_9 = \frac{Gr}{r_2^2-r_2-\frac{1}{K}(1+M)}$$

$$M_{10} = \frac{GcM_5}{r_6^2-r_6-\frac{1}{K}(1+M)} \qquad M_{11} = \frac{GcM_4}{r_2^2-r_2-\frac{1}{K}(1+M)}$$

$$M_{12} = U_p + M_9 + M_{10} - M_8 - M_{11} \qquad M_{13} = M_{11} - M_9$$

$$M_{14} = \frac{Gr}{r_4^2-r_4-M_1} \qquad M_{15} = \frac{GcM_7}{r_8^2-r_8-M_1}$$

$$M_{16} = \frac{GcM_6}{r_4^2-r_4-M_1} \qquad M_{17} = M_{14} + M_{15} - M_{16}$$

$$M_{18} = M_{16} - M_{14}$$

References

[1] Shercliff J. A., A Text Book of Magnetohydrodynamics, Pergamon Press, London. (1965).

[2] Ferraro V.C.A., Plumpton C., An introduction to Magneto Fluid Mechanic, Clarandon press, Oxford. (1966).

[3] Crammer K.P. and Pai S.L., Magneto-fluid Dynamic for Engineers and Applied Physicist, Mc-Graw Hill book Co, New York. (1973).

[4] Raptis A. A., Flow through a porous medium in the presence of magnetic field, International journal of Energy Research, 10(1) (1986), 97- 100.

[5] Singh K. D., Hydromagnetic effects on the three-dimensional flow past a porous plate, ZAMP, 41 (1990), 441-446.

[6] Brevster M. Q., Thermal radiation transfer and properties, John while and sons, New Yorck, NY, USA. (1992).

[7] Raptis A. and Perdikis C., Unsteady flow through a highly porous medium in the presence of radiation, Transport in Porous Media, 57(2) (2004), 171-179.

[8] Varshney N. K. and Prakash Ram, MHD effect on three-dimensional free convective flow with heat transfer through a porous medium with periodic permeability, Ganita, 55(1) (2004), 75.

[9] Ibrahim S. M., Radiation effects on mass transfer flow through a highly porous medium with heat generation and chemical reaction, ISRN Computational Mathematics, Article ID 765408,2013, 9.

[10] Rani K. Jhansi, Reddy G.V., Ramana Murthy, Ch. V. Ramana and Murthy M. V. Ramana, Heat and mass transfer effects on mhd free convection flow over an inclined plate embedded in a porous medium, Int. J. Chem. Sci., 13(4) (2015), 1998-2016 ISSN 0972-768X.

[11] Paul Ashish, Transient Free Convective MHD Flow past an Exponentially Accelerated Vertical Porous Plate with Variable Temperature through a Porous Medium, International Journal of Engineering Mathematics, Article ID 2981071, 2017, 9.

[12] Goud B. Shankar and Shekar M. N. Raja, Finite element study of Soret and radiation effects on mass transfer flow through a highly porous medium with heat generation and chemical reaction, International Journal of Computational and Applied Mathematics, 12(1) (2017), 53-64.

[13] Suneetha K., Ibrahim S. Mohammed and Reddy G. V. Ramana Reddy, A study on free convective heat and mass transfer flow through a highly porous medium with radiation, chemical reaction and Soret effects, JCARME, 8(2) (2018), 121-132.

[14] Ramakrishnan K., Combined effects of Slip parameter and Inclined magnetic field on MHD flow through two infinite parallel plates filled by porous medium, International Journal of Pure and Applied Mathematics, 118(11) (2018), 61-69.